3 November 2025

Cosolvents Disrupt Water H-bond Networks at Electrode Interfaces: a Surface-enhanced 2D IR Study

Saptarsi Mondal[1], Kevin Chen[1], Carlos Baiz[1]

1. The University of Texas at Austin

Abstract

Picosecond electric field fluctuations mediate local environments that govern electrocatalysis at the electrode-water interface. Consequently, cosolvents modulate hydrogen-bond networks and interfacial dynamics. Here, we use surface-enhanced two-dimensional infrared (SE 2D IR) spectroscopy to quantify the effect of the cosolvent dimethyl sulfoxide (DMSO) on water dynamics by measuring the picosecond frequency fluctuation timescales of nitrile-based vibrational probes at a functionalized gold surface to extract H-bond lifetimes. We find that DMSO considerably accelerates interfacial H-bond rearrangements. In contrast, DMSO slows dynamics in the bulk, consistent with long-lived water-DMSO microdomains. The interface vs bulk comparison shows that DMSO disrupts cooperative H-bonding of water by inducing disorder at the interface, speeding up H-bond rearrangements, whereas in a bulk environment, long-lived microheterogeneity exhibits slower dynamics. The study demonstrates that bulk properties rarely reflect the interface highlighting the complexities of predicting solvent behavior at electrochemical interfaces. The results indicate that cosolvents can modulate local dynamics and offer extra control over interfacial properties.

Keywords

2D IR spectroscopy, ultrafast, hydrogen bond, electrochemical interfaces

MANUSCRIPT

Cosolvents Disrupt Water H-bond Networks at Electrode Interfaces: A Surface-enhanced 2D IR Study

Saptarsi Mondal, Kevin Chen, Carlos R. Baiz*

Department of Chemistry, University of Texas at Austin, Austin, TX 78712, USA

**Corresponding author: cbaiz@cm.utexas.edu*

Abstract:

Picosecond electric field fluctuations mediate local environments that govern electrocatalysis at the electrode-water interface. Consequently, cosolvents modulate hydrogen-bond networks and interfacial dynamics. Here, we use surface-enhanced two-dimensional infrared (SE 2D IR) spectroscopy to quantify the effect of the cosolvent dimethyl sulfoxide (DMSO) on water dynamics by measuring the picosecond frequency fluctuation timescales of nitrile-based vibrational probes at a functionalized gold surface to extract H-bond lifetimes. We find that DMSO considerably accelerates interfacial H-bond rearrangements. In contrast, DMSO slows dynamics in the bulk, consistent with long-lived water-DMSO microdomains. The interface vs bulk comparison shows that DMSO disrupts cooperative H-bonding of water by inducing disorder at the interface, speeding up H-bond rearrangements, whereas in a bulk environment, long-lived microheterogeneity exhibits slower dynamics. The study demonstrates that bulk properties rarely reflect the interface highlighting the complexities of predicting solvent behavior at electrochemical interfaces. The results indicate that cosolvents can modulate local dynamics and offer extra control over interfacial properties.

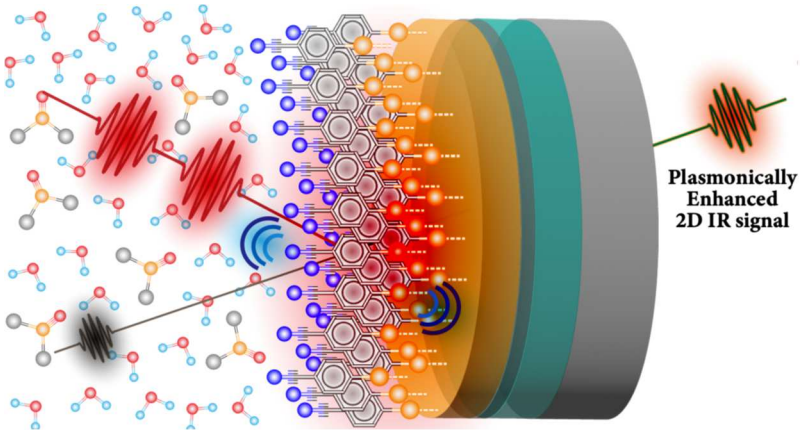

Table of Contents Graphic

Introduction

In confined or interfacial environments, water H-bond structures and dynamics can deviate significantly from the bulk as a result of a constrained conformational space.[1-2] Solid-liquid interfaces in particular confine water to a quasi-two-dimensional layer, which fundamentally alters H-bonding networks and dynamics.[3] Electrochemical interfaces are a prime example: molecular orientations are influenced by surface chemistry and interfacial electric fields, with direct implications for reaction rates and mechanisms.[4-5] Indeed, recent studies based on two-dimensional infrared spectroscopy (2D IR) showed that applied voltages can modulate the H-bond dynamics of water at functionalized electrode surfaces.[6-7] For instance, water donating a H-bond to a nitrile-terminated monolayer was found to break and reform its H-bond ~2–3× slower under a positive electrode bias (i.e. a "locked" H-bond network) than under a negative bias (i.e. a "labile" H-bond network), emphasizing the sensitivity of interfacial H-bond networks to external perturbations like local electric fields.

Cosolvents provide an alternative means to control water's H-bond networks both at the interface and in bulk. For example, dimethyl sulfoxide (DMSO) is a widely used cosolvent and cryoprotectant that disrupts the H-bond donor-acceptor balance, reshaping the H-bond network.[8-11] In bulk, DMSO induces clustering, H-bond disorder, and local microheterogeneity, resulting in bulk properties that significantly deviate from ideality.[9] DMSO–water mixtures tend to form DMSO-rich and water-rich domains.[8-9] Bulk dynamics exhibit two time scales: a fast ~1 ps component associated with local H-bond fluctuations, referred to as in-place inertial fluctuations, and a slower tens-of-ps component associated with H-bond making/breaking and global network rearrangement.[12] Notably, bulk water-DMSO mixtures exhibit non-monotonic changes in H-bond dynamics with increasing DMSO concentration, segregate into domains above 30 mol%, creating local disorder.[12] This complex behavior in bulk prompts the question: how would the same cosolvent affect water at an interface where the conformational space is more constrained?

In this work, we focus on DMSO's influence on interfacial water at a gold surface with a covalently tethered nitrile-terminated monolayer (4-mercaptobenzonitrile, 4-MBN). The C≡N stretching vibration is a useful reporter of local solvation and H-bonding environments. Surface-enhanced 2D IR (SE 2D IR) spectroscopy of the nitrile stretch mode probes how DMSO modulates water's H-bond dynamics (i.e. H-bond lifetimes) to the nitrile group. We show that DMSO acts as a

"network disruptor" for water, but the consequences of disrupting the H-bond network differ between the constrained 2D interfacial environment and 3D bulk environments. Below, we discuss these mechanisms in detail and explore implications for electrochemical interfaces.

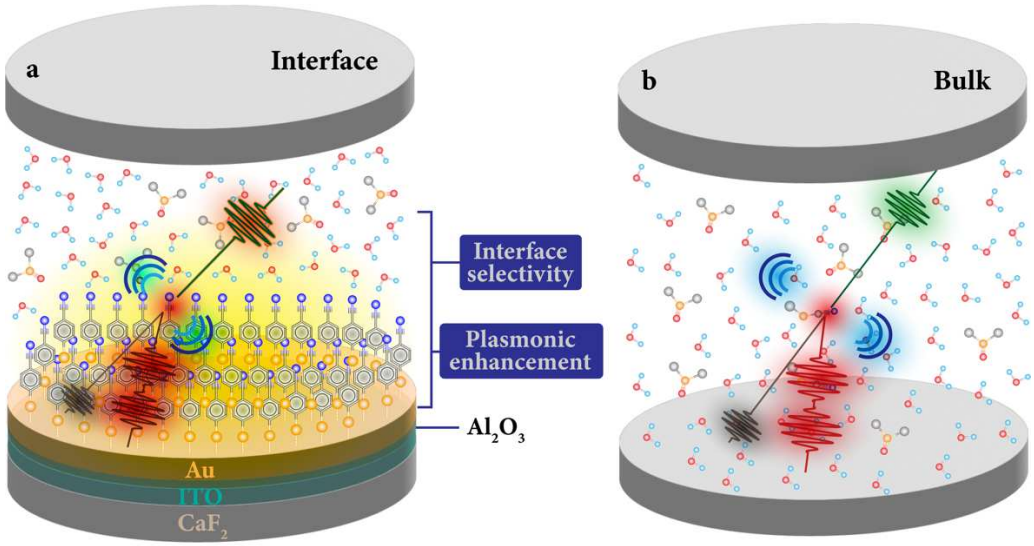

Figure 1. Scheme of surface-enhanced 2D IR spectroscopy of the nitrile mode of the 4-mercaptobenzonitrile functionalized Au electrode. (a). The nitrile stretch mode acts as a sensitive reporter of local solvation and H-bonding environment. The 2D IR signal is enhanced by the Au plasmons. The Indium-doped tin oxide (ITO) layer prevents Fano-type distortions of the 2D IR signal due to its interference with the gold plasmon band, whereas the Al_2O_3 layer acts as the resistive layer. The scheme of bulk-allowed 2D IR spectroscopy of the -SCN stretch mode in solutions (b). Here, the nitrile probes are dissolved at low concentrations in the bulk cosolvent mixtures.

Results

Interfacial dynamics

We employed a plasmonic electrochemical cell with covalently-tethered surface vibrational labels (Figure 1), producing an enhanced signal from the interface without spectral distortion.[6-7] Specifically, a 4-MBN self-assembled monolayer was covalently tethered to the gold.[13] This platform enables probing interfacial dynamics in transmission-mode 2D IR.[6] In this study, all measurements were conducted in the absence of an applied electric field.

We first consider the 2D IR spectra of the nitrile stretch at the interface. Figure 2 shows selected 2D IR spectra for pure water, 5 mol%, and 20 mol% DMSO in the DMSO-water binary cosolvent mixtures at two waiting times for the interface, and Figure 3 shows corresponding spectra for the bulk whereas all the 2D IR spectra along with pump slice, probe slice, diagonal slice and pump slice amplitude (PSA) spectra at various waiting times and chemical compositions are presented in Figure S1-S12. To quantify the timescales of nitrile frequency fluctuations (spectral diffusion), we performed a center line slope (CLS) analysis of the diagonal peak.[14-15] In brief, CLS tracks how quickly the correlation between initial and final vibrational frequencies decays as a function of waiting time t_2.[14-17] A slope of one indicates full frequency correlation corresponding to no frequency change, whereas a slope of zero indicates complete loss of memory (i.e., the frequency becomes fully randomized).[15] The CLS dynamics exhibit multi-exponential behavior. For example, in pure water, a fast component of 0.93 ps and a slower component of 9.90 ps are observed (Figure 4A, Figure 5). Following previous interpretations based on experiments and MD simulations, the fast component corresponds to local H-bond fluctuations without H-bond switching.[6-7] Fast dynamics include in-place wobbling and H-bond stretching, analogous to the fast *local* spectral diffusion seen for HOD in bulk water.[18] The slow component, by contrast, corresponds directly to the activated H-bond formation and breaking. The bi-exponential CLS behavior thus represents the two physical regimes: rapid local fluctuations (~1 ps) and slower H-bond lifetimes (tens of ps).[6-7]

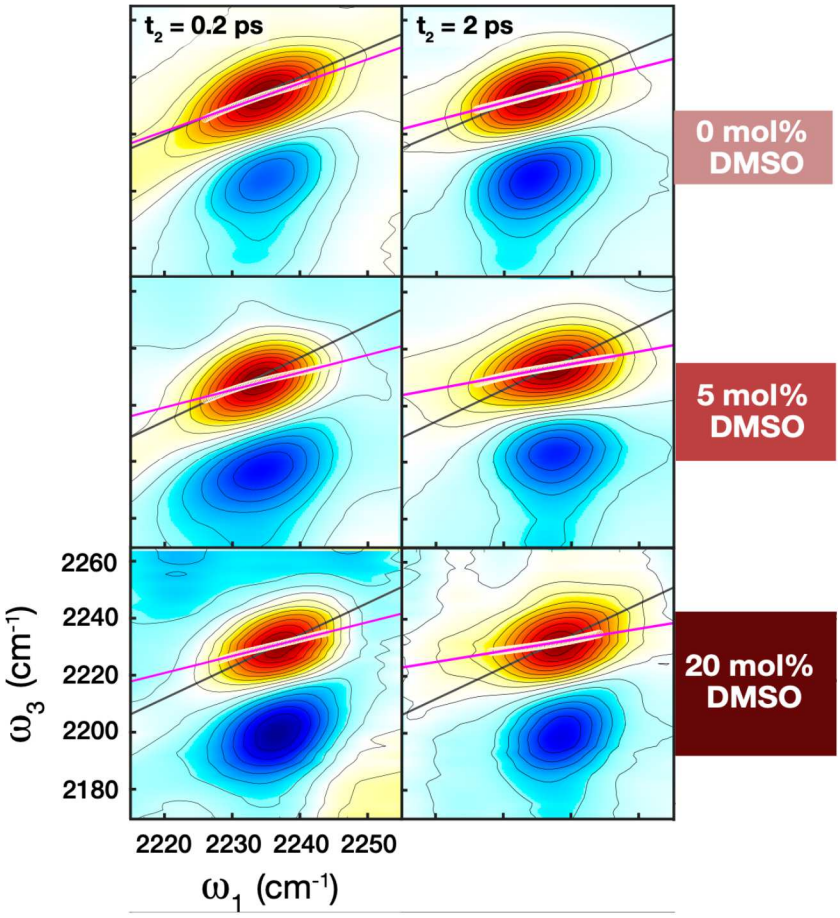

Figure 2. Example SE 2D IR spectra of the nitrile stretch mode of 4-MBN functionalized Au interface for pure water, 5 and 20 mol% DMSO in the DMSO-water binary cosolvent mixture at two selected waiting times. The CLS is shown in white, with a linear fit in magenta.

The addition of DMSO induces changes in the spectral diffusion timescales. Notably, at the interface, DMSO induces significant acceleration of the slow, H-bond making/breaking component. Even with 5 mol% DMSO, a notably faster decay of 5.56 ps compared to pure water at ~9.9 ps, and at 20 mol% DMSO, the slow component further decreases to 1.84 ps (Figure 5). In general, increasing the DMSO fraction leads to systematically shorter H-bond lifetimes at the interface. In contrast, the fast ~1 ps component remains essentially unchanged with DMSO addition. This selective influence of DMSO on the slow exchange dynamics, but not on the ultrafast inertial dynamics, is a key observation, indicating that DMSO primarily affects the *cooperative* rearrangements of the H-bond network, rather than in-place inertial fluctuations. In fact, the invariance of the fast component suggests that water undergoes picosecond-scale

fluctuations while interacting with DMSO almost as freely as having another water as a neighbor. In contrast, the H-bond exchange lifetime becomes faster with increasing DMSO concentration. Namely, the nitrile reporter samples various H-bond populations very quickly, resulting in faster frequency decorrelation. It is worth noting that spectra do not exhibit distinct peaks for "DMSO-contact" vs "water-contact" nitriles; instead, the nitrile lineshapes remain unimodal, with DMSO. Furthermore, while we report bulk concentrations, it is worth noting that interfacial DMSO concentrations are significantly higher than bulk. For example, on bare gold, there is a 4× enrichment, meaning that 5 mol% DMSO in bulk results in 20 mol% at the interface,[19], which explains the pronounced effects even at "dilute" concentrations. In summary, at the interface, DMSO causes the nitrile's frequency to lose memory of its starting value much faster, due to faster H-bond rearrangements, while the local fluctuations remain largely unchanged.

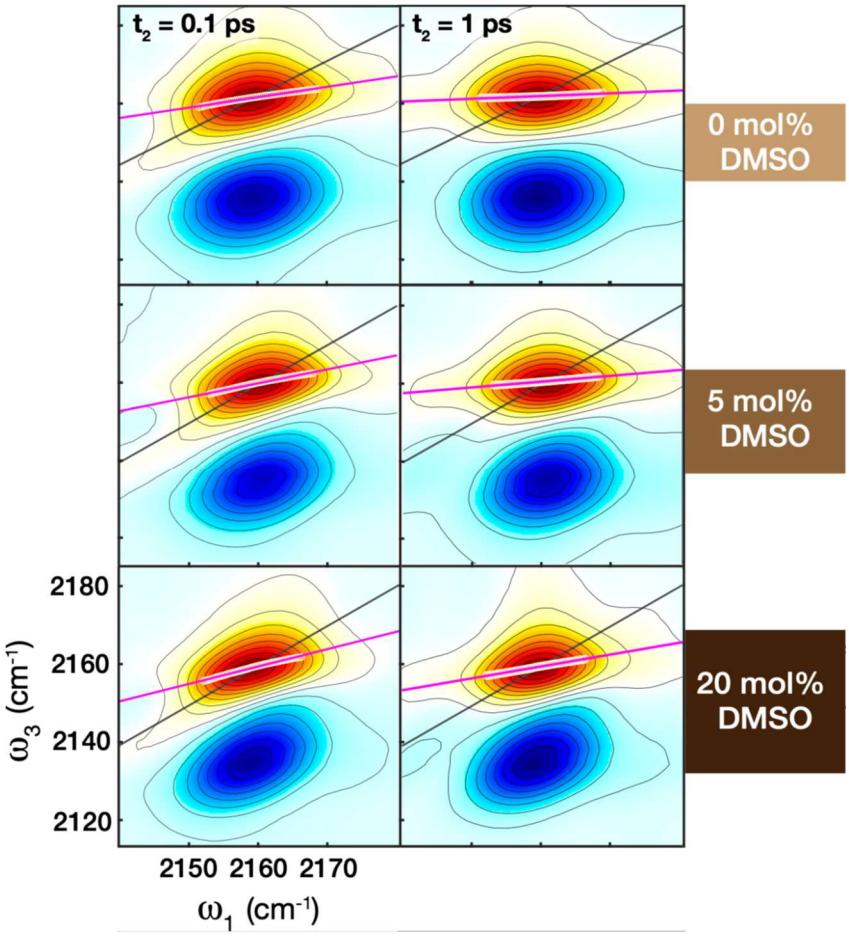

Figure 3. Example bulk 2D IR spectra of the nitrile stretch mode of MeSCN for pure water, 5 and 20 mol% DMSO in the DMSO-water binary cosolvent mixture at two selected waiting times. The CLS is shown in white, with a linear fit in magenta.

Bulk dynamics

To understand the differences between interfacial and bulk DMSO effects, we additionally measured 2D IR of the nitrile stretch in methyl thiocyanate (MeSCN) in the same co-solvent solutions (Figure 3 and Figure S14-S28). MeSCN is similarly sensitive to H-bonding: water can donate an H-bond to the nitrile, whereas DMSO's lack of polar hydrogens prevents direct H-bond interactions with the nitrile. In pure water, the MeSCN nitrile stretch mode experiences an essentially homogeneous environment, and its 2D IR CLS decays on a ~1 ps timescale, consistent with previous measurements.[12] Introducing DMSO into the bulk slows the spectral diffusion and also introduces signs of dynamic heterogeneity. Up to 5 mol% DMSO, the dynamics follow single-exponential relaxation with a modest increase in relaxation time (Figure 5, Table S1). In mixtures such as 10, 20, or 30 mol% DMSO, the CLS decays of MeSCN develop a bi-exponential character similar to the interface: a fast component (~1–2 ps) assigned to local fluctuations, and a slow component (~5–10 ps) that grows in amplitude with increasing DMSO concentration (Table S1). Analogous to interfacial dynamics, the slow component is attributed to H-bond exchange. [12] The measured dynamics in bulk solution are consistent with earlier ultrafast studies.[9]

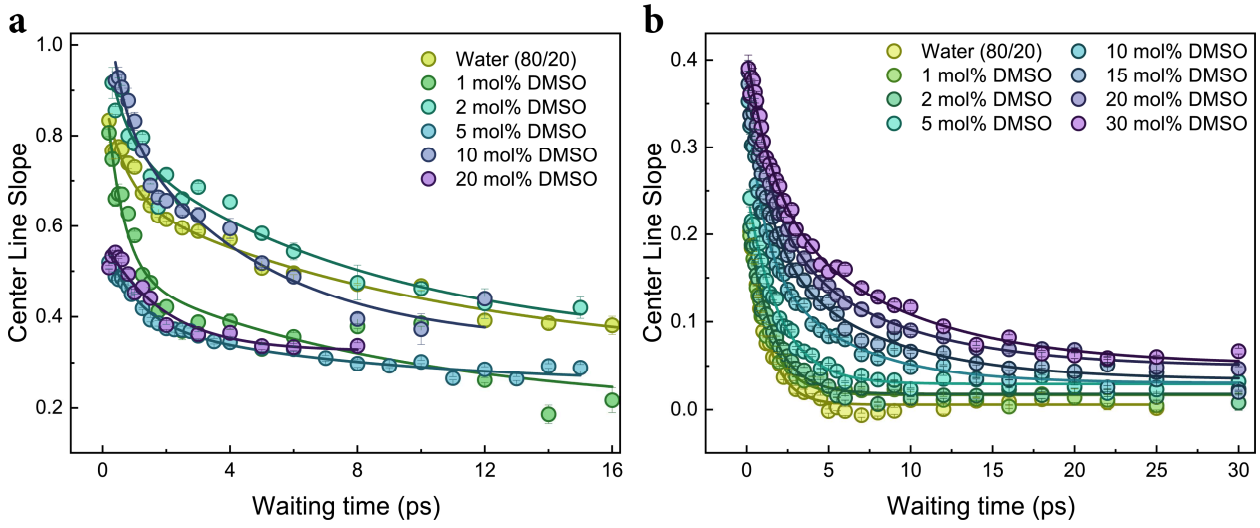

Figure 4. Center line slope (CLS) decay extracted from (a) SE 2D IR spectra of the nitrile stretch mode of 4-MBN functionalized Au interface and corresponding fitting with biexponential function, (b) bulk 2D IR peak of the nitrile stretch mode of MeSCN in solutions.

In bulk, the slow spectral diffusion component (reflecting global H-bond network reorganization) tracks the slow orientational relaxation time and slow nanoscopic length scale diffusion of water.[12] In the present studies, at 20 mol% DMSO, the slow CLS component for MeSCN decays on the ~5–10 ps timescales, significantly slower than pure water. Furthermore, unlike the interface, there is evidence of more *static* heterogeneity in bulk: the pump slice spectra of MeSCN in certain DMSO-rich mixtures show slight broadening, hinting at the presence of multiple sub-ensembles (Figure S26, S28), supporting the presence of distinct "clusters". Spectra show a single nitrile peak, suggesting that the shift is not sufficiently large to be resolved. Importantly, changes in dynamics with DMSO are opposite at the interface versus in bulk: The slow H-bond correlation time decreases by roughly a factor of 5 from 0 to 20% DMSO at the interface, whereas it increases by almost a factor of 8 in the bulk over the same composition range. On the other hand, the fast component remains ~1 ps in all cases, with only minor (~20%) variations in either environment. These results demonstrate that DMSO's impact is concentrated on the collective, long-timescale rearrangement of the H-bond network, accelerating H-bond exchange at the constrained interfacial environments but slowing the same processes in bulk.

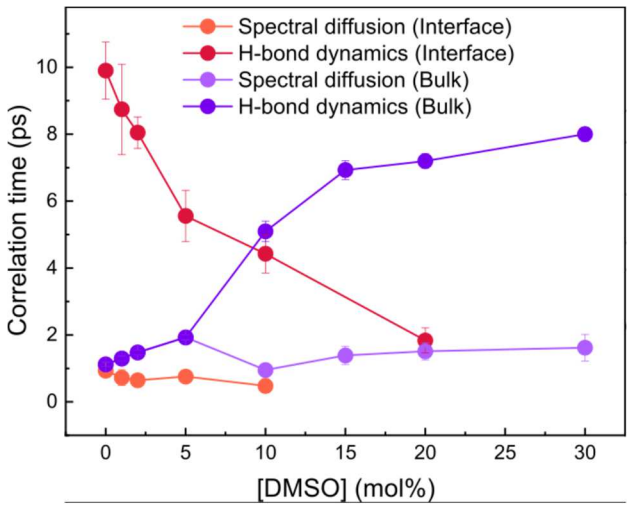

Figure 5. Single or biexponential fitting parameters extracted from spectral diffusion (~1 ps) and H-bond exchange (~4-10 ps) timescales of nitrile stretch mode at the interface as a function of DMSO concentration in the binary mixture compositions studied here. The values are reported in Table S1.

We report population relaxation dynamics (vibrational lifetime) of the nitrile stretch mode at the interface and the bulk for various chemical compositions which can be found in Figure S29 with corresponding single or biexponential fitting parameters in Table S2. The vibrational lifetime of

the nitrile stretch mode is around 7-10 ps for 4-MBN at the interface and 25-35 ps for MeSCN in solution (bulk) suggesting that nitrile stretch mode remain largely insensitive to the chemical composition changes.

Discussion

DMSO as a hydrogen-bond breaker: interfacial versus bulk

Understanding DMSO's "dual personality" lies in how interfacial confinement disrupts water H-bond networks. In a bulk mixture, water initially satisfies the H-bond imbalance by directly H-bonding with DMSO, and at higher concentrations, water and DMSO undergo phase separation, yielding a heterogeneous environment.[9, 20] DMSO increases the solution viscosity and can form stabilizing one-DMSO–two-water complexes. The result is a slowdown of processes that require reorganizing the H-bond network. The slow spectral diffusion component in bulk is precisely this: the timescale for a probe's environment to become thoroughly randomized by H-bond exchange. The current observations and interpretations are consistent with previous studies showing H-bond exchange in ~5-10 picoseconds in intermediate DMSO mixtures.[6]

In contrast, at the 4-MBN/Au interface, H-bond exchange involves a few molecular layers adjacent to the surface.[6] The monolayer of closely packed 4-MBN presents polar nitrile groups. Interfacial water is inherently constrained and undercoordinated in this environment.[21-22] This under-coordination means H-bond making/breaking has lower activation barriers than bulk. Furthermore, DMSO within the interfacial environment acts additional H-bond acceptor, thus competing with the nitriles. In bulk, water-water interactions produce an extended network leading to fast dynamics; on the other hand, at the interface, H-bond switching involves long-range reorganization. In essence, DMSO's presence at the interface introduces H-bond "holes" or weak links in the network that significantly shorten the H-bond rearrangement time scale, which explains the observed spectral diffusion with DMSO at the interface. This effect is amplified further by the enrichment of DMSO at the interface.[19, 23]

Dimensionality and electric fields: towards controlling interfacial dynamics.

It is useful to draw analogies between the present cosolvent-induced effect and the effect of an applied electric field. Recent SE 2D IR studies reported that negative electrode potentials (excess electrons on Au) tend to destabilize water's interfacial H-bonding and accelerate its short-time dynamics. A negative bias (–0.2 V) shortened the water–nitrile H-bond lifetime to ~25 ps from ~60 ps at +0.3 V vs Ag/AgCl. In our study, adding DMSO at open-circuit-potential achieved a comparable effect, where H-bond dynamics become ~5× faster in 20 mol% DMSO compared to pure water. In essence, DMSO qualitatively mimics the effect of applying a substantial negative bias: in both cases, the interfacial water network becomes more labile and H-bonds exchange faster.

This convergence is remarkable given that DMSO is an electrically neutral molecule. It suggests that cosolvent effects can substitute for electrostatic effects in tuning interfacial solvent properties. From a practical standpoint, in scenarios where large potentials are undesirable due to competing reactions or electrode degradation, using a cosolvent could be an alternative strategy to modulate the interface. We emphasize, however, that cosolvents and electric fields are not the same: a field also organizes the double-layer ions and orients dipoles, whereas cosolvents alter interfacial compositions and can also directly interact with solutes.[24] The ability to tune water's H-bond dynamics by altering chemical compositions could have implications for electrochemical reaction rates. Many reactions at electrodes involve water as a reactant, product, or proton shuttle, such as the hydrogen evolution reaction (HER) and CO_2 reduction reaction (CO_2RR).[25-31] A rigid, strongly H-bonded interfacial water layer can stabilize certain intermediates through strong electrostatic interactions, but it may also impede the rapid reorganization needed for proton transfer or diffusion. Conversely, a more disordered, fast-moving water layer may facilitate proton hopping and adaptation of the solvation shell during multi-step reactions.[29] Our findings suggest that adding DMSO yields a more "fluxional" solvation environment akin to a negatively charged interface. Notably, recent work has shown that cosolvents influence product ratios in the CO_2 reduction reaction.[32] Microdomains at the interface could cause certain reaction intermediates to phase separate selectively.[33]

Concluding Remarks

The current study demonstrates that the interfacial solvation can be tuned chemically. Using SE 2D IR with a nitrile reporter, we showed that low DMSO concentrations markedly accelerate interfacial H-bond exchange while the same cosolvent slows bulk structural diffusion. We attribute this inversion to the combination of reduced dimensionality, H-bond lifetime, interfacial enrichment of an H-bond acceptor-only cosolvent, and the resulting loss of H-bond cooperativity within the quasi-2D water layer. Essentially, cosolvent composition serves as an additional degree of freedom, complementary to applied potential, for tuning interfacial solvation dynamics relevant to proton/hydroxide transfer and stabilization of reactive intermediates. By establishing a clear, quantitative link between cosolvent chemical properties and interfacial H-bond lifetimes, this study lays the groundwork for chemically altering the electric double-layer properties. We anticipate that coupling chemical composition with potential will enable rational, mV-level tuning of interfacial dynamics to enhance selectivity and rates in electrocatalytic reactions.

Materials and Methods

Sample Preparation: Au-coated plasmonic working electrodes were purchased from PhaseTech Spectroscopy. In brief, the cells consist of an indium tin oxide (ITO) layer (~15 nm), an Al_2O_3 tunnel barrier (3–4 nm), and a thin gold film (~3 nm) on an IR-transparent CaF_2 substrate.[15] The ITO allows for electrical conductivity and serves as a base electrode, while the ultrathin Au film produces the surface-plasmon enhancement.[6-7] A monolayer of 4-mercaptobenzonitrile (4-MBN) was assembled on the gold surface by immersing the substrate in a 1 mM solution of 4-MBN in ethanol for >12 h, then rinsing with ethanol. The densely packed 4-MBN monolayer ensures that all nitrile groups are oriented outward and exposed to the solution. Windows were pressed together with no spacers to reduce the water background signal in 2D IR measurements, producing a liquid thickness of ~6 μm between windows. No external voltage was applied to the electrochemical system. All solutions were prepared with 80% deionized water (Milli-Q) and 20% D_2O along with spectroscopy-grade DMSO. For bulk 2D IR experiments of MeSCN (0.7 M), a 25 μm spacer was used between two IR-transparent CaF_2 windows.

2D IR Spectroscopy: The 2D IR spectrometer was described previously.[34] Briefly, mid-IR pulses (~100 fs duration, 1 kHz repetition rate) centered at 2230 cm^{-1} (for 4-MBN) and at 2160 cm^{-1} (for MeSCN probe) were generated via a combination of optical parametric amplification using type II BBO crystals and difference frequency generation using $AgGaS_2$. A standard pump–probe geometry was employed to acquire 2D IR spectra. Two pump pulses arranged in a collinear pump sequence with a controlled delay generated by a pulse shaper (PhaseTech Spectroscopy) excited the sample, and a weaker, time-delayed probe pulse sampled the induced vibrational coherence. The absorptive 2D IR signal was detected on a dispersive 128x128 element mid-IR MCT array. The 0-1 and 1-2 transition of the nitrile appears as a pair of lobes (absorptive line shape) along the diagonal. Notably, the monolayer signals are enhanced by the plasmonic Au island film, yielding strong nonlinear signals despite the monolayer coverage.[7]

Center Line Slope (CLS) Analyses: Spectral diffusion was quantified via the CLS method.[14-15] For each waiting time t_2, a "center line" was obtained by tracing the maximum of the 2D peak along the detection axis ω_3. The slope of this line provides a normalized frequency–frequency correlation function $C_2(t)$. The CLS values were plotted as a function of t_2 and fit to a bi-exponential decay function:

$$C(t_2) = A_{fast} exp^{\left(-\frac{t_2}{\tau_{fast}}\right)} + A_{slow} exp^{\left(-\frac{t_2}{\tau_{slow}}\right)} + \mathrm{C}(\infty)$$

The fast time constant τ_{fast} captures the initial fast drop in CLS (frequency memory loss due to local fluctuations), while τ_{slow} captures the long-time decay to zero (memory loss due to complete environmental reorganization). In our analysis, τ_{fast} was ~0.8–1.2 ps for all samples, bulk and interface, with little systematic change upon DMSO addition, whereas τ_{slow} varied strongly with DMSO fraction and environment. The fitting also yields the amplitudes A_{fast} and A_{slow} and an offset (Table S1) We found A_{slow} (fraction of slow-decaying component) increased with DMSO in bulk, but decreased with DMSO at the interface, reflecting the growing or shrinking population of distinct long-lived states in each scenario, respectively. Uncertainty in the extracted τ_{slow} is on the order of ± 0.4 to ± 0.8 ps for interface data and ± 0.2 to ± 0.3 ps for bulk data at various compositions, based on a bootstrapping method.[35]

Supplementary Materials.

The detailed CLS analyses of the nitrile stretch mode at the interface and the bulk at various waiting times, t_2, can be found in the Supporting Information along with pump-slice, probe slice, diagonal slice spectra, and pump-slice amplitude spectra across the range of compositions at the interface and the bulk. The fitting parameters extracted from biexponential fitting with an offset can also be found in the SI.

Acknowledgements

This work was funded by the Department of Energy (DE-SC0023221) and the Welch Foundation (F-1891). The authors thank Dr. Ziareena Al-Mualem for performing initial tests of the spectroelectrochemical cells.

References

1. Gonella, G.; Backus, E. H. G.; Nagata, Y.; Bonthuis, D. J.; Loche, P.; Schlaich, A.; Netz, R. R.; Kühnle, A.; McCrum, I. T.; Koper, M. T. M.; Wolf, M.; Winter, B.; Meijer, G.; Campen, R. K.; Bonn, M., Water at charged interfaces. *Nat. Rev. Chem.* **2021,** *5* (7), 466-485.

2. de la Puente, M.; Laage, D., Impact of interfacial curvature on molecular properties of aqueous interfaces. *J. Chem. Phys.* **2024,** *160* (23).

3. Groß, A.; Sakong, S., Ab Initio Simulations of Water/Metal Interfaces. *Chem. Rev.* **2022,** *122* (12), 10746-10776.

4. Nauman, J. A.; Suvlu, D.; Willard, A. P., Electric Fields at Solid-Liquid Interfaces: Insights from Molecular Dynamics Simulation. *Annu. Rev. Phys. Chem.* **2025,** *76* (Volume 76, 2025), 181-202.

5. Speelman, R.; Marker, E. J.; Boamah, M. D.; Kupferberg, J.; Bye, J. Z.; Engelhard, M.; Zhao, Y.; Martinson, A. B.; Rosso, K. M.; Geiger, F. M., Water flipping and the oxygen evolution reaction on Fe2O3 nanolayers. *Nature communications* **2025,** *16* (1), 3585.

6. Ryan, M. J.; Yang, N.; Kwac, K.; Wilhelm, K. B.; Chi, B. K.; Weix, D. J.; Cho, M.; Zanni, M. T., The hydrogen-bonding dynamics of water to a nitrile-functionalized electrode is modulated by voltage according to ultrafast 2D IR spectroscopy. *Proc. Natl. Acad. Sci. U.S.A.* **2023,** *120* (52), e2314998120.

7. Yang, N.; Ryan, M. J.; Son, M.; Mavrič, A.; Zanni, M. T., Voltage-Dependent FTIR and 2D Infrared Spectroscopies within the Electric Double Layer Using a Plasmonic and Conductive Electrode. *J. Phys. Chem. B* **2023,** *127* (9), 2083-2091.

8. Venkatraman, R. K.; Baiz, C. R., Ultrafast Dynamics at the Lipid–Water Interface: DMSO Modulates H-Bond Lifetimes. *Langmuir* **2020,** *36* (23), 6502-6511.

9. Oh, K.-I.; You, X.; Flanagan, J. C.; Baiz, C. R., Liquid–Liquid Phase Separation Produces Fast H-Bond Dynamics in DMSO–Water Mixtures. *J. Phys. Chem. Lett.* **2020,** *11* (5), 1903-1908.

10. Banerjee, S.; Roy, S.; Bagchi, B., Enhanced Pair Hydrophobicity in the Water−Dimethylsulfoxide (DMSO) Binary Mixture at Low DMSO Concentrations. *J. Phys. Chem. B* **2010,** *114* (40), 12875-12882.

11. Luzar, A.; Chandler, D., Structure and hydrogen bond dynamics of water–dimethyl sulfoxide mixtures by computer simulations. *J. Chem. Phys.* **1993,** *98* (10), 8160-8173.

12. Wong, D. B.; Sokolowsky, K. P.; El-Barghouthi, M. I.; Fenn, E. E.; Giammanco, C. H.; Sturlaugson, A. L.; Fayer, M. D., Water Dynamics in Water/DMSO Binary Mixtures. *J. Phys. Chem. B* **2012,** *116* (18), 5479-5490.

13. Kwac, K.; Yang, N.; Ryan, M. J.; Zanni, M. T.; Cho, M., Molecular dynamics simulation study of water structure and dynamics on the gold electrode surface with adsorbed 4-mercaptobenzonitrile. *J. Chem. Phys.* **2024,** *160* (6).

14. Hoffman, D. J.; Fica-Contreras, S. M.; Fayer, M. D., Fast dynamics of a hydrogen-bonding glass forming liquid: Chemical exchange-induced spectral diffusion in 2D IR spectroscopy. *J. Chem. Phys.* **2019,** *150* (12).

15. Guo, Q.; Pagano, P.; Li, Y.-L.; Kohen, A.; Cheatum, C. M., Line shape analysis of two-dimensional infrared spectra. *J. Chem. Phys.* **2015,** *142* (21).

16. Baiz, C. R.; Błasiak, B.; Bredenbeck, J.; Cho, M.; Choi, J.-H.; Corcelli, S. A.; Dijkstra, A. G.; Feng, C.-J.; Garrett-Roe, S.; Ge, N.-H.; Hanson-Heine, M. W. D.; Hirst, J. D.; Jansen, T. L. C.; Kwac, K.; Kubarych, K. J.; Londergan, C. H.; Maekawa, H.; Reppert, M.; Saito, S.; Roy, S.; Skinner, J. L.; Stock, G.; Straub, J. E.; Thielges, M. C.; Tominaga, K.; Tokmakoff, A.; Torii, H.; Wang, L.; Webb, L. J.; Zanni, M. T., Vibrational Spectroscopic Map, Vibrational Spectroscopy, and Intermolecular Interaction. *Chem. Rev.* **2020,** *120* (15), 7152-7218.

17. Kim, Y. S.; Hochstrasser, R. M., Chemical exchange 2D IR of hydrogen-bond making and breaking. *Proc. Natl. Acad. Sci. U.S.A.* **2005,** *102* (32), 11185-11190.

18. Eaves, J. D.; Loparo, J. J.; Fecko, C. J.; Roberts, S. T.; Tokmakoff, A.; Geissler, P. L., Hydrogen bonds in liquid water are broken only fleetingly. *Proc. Natl. Acad. Sci. U.S.A.* **2005,** *102* (37), 13019-13022.

19. Al-Mualem, Z. A.; Lorenz-Ochoa, K. A.; Pan, L.; Ren, H.; Baiz, C. R., Controlling Interfacial Hydrogen Bonding at a Gold Surface: The Effect of Organic Cosolvents. *J. Phys. Chem. Lett.* **2024,** *15* (16), 4391-4399.

20. Oh, K.-I.; Rajesh, K.; Stanton, J. F.; Baiz, C. R., Quantifying Hydrogen-Bond Populations in Dimethyl Sulfoxide/Water Mixtures. *Angewandte Chemie International Edition* **2017,** *56* (38), 11375-11379.

21. Ni, Y.; Gruenbaum, S. M.; Skinner, J. L., Slow hydrogen-bond switching dynamics at the water surface revealed by theoretical two-dimensional sum-frequency spectroscopy. *Proc. Natl. Acad. Sci. U.S.A.* **2013,** *110* (6), 1992-1998.

22. Shi, L.; LaCour, R. A.; Qian, N.; Heindel, J. P.; Lang, X.; Zhao, R.; Head-Gordon, T.; Min, W., Water structure and electric fields at the interface of oil droplets. *Nature* **2025,** *640* (8057), 87-93.

23. Mondal, S.; Al-Mualem, Z. A.; Cardenas, A. E.; Hazarika, S.; Lee, H.; Ren, H.; Baiz, C. R., Tuning Hydrogen Bond Networks at Gold Electrodes: A Study of Potential-Dependent DMSO–Water Interfaces. *ACS Electrochem.* **2025,** *1* (5), 709-717.

24. Speelman, R.; Marker, E. J.; Geiger, F. M., Quantifying Stern layer water alignment before and during the oxygen evolution reaction. *Sci. Adv.* **2025,** *11* (10), eado8536.

25. Cheng, Y.; Li, Q.; Salaman, M. I. B.; Wei, C.; Wang, Q.; Ma, X.; Liu, B.; Wong, A. B., Microenvironment Tailoring for Electrocatalytic CO2 Reduction: Effects of Interfacial Structure on Controlling Activity and Selectivity. *J. Am. Chem. Soc.* **2025,** *147* (15), 12438-12448.

26. Winkler, D.; Leitner, M.; Auer, A.; Kunze-Liebhäuser, J., The Relevance of the Interfacial Water Reactivity for Electrochemical CO Reduction on Copper Single Crystals. *ACS Catal.* **2024,** *14* (2), 1098-1106.

27. Jiang, L.; Zhou, C.; Cai, J.; Li, K.; Wang, H., Water-mediated reduction of carbon dioxide. *Cell Rep.* **2024,** *5* (10), 102246.

28. Mohandas, N.; Narayanan, T. N.; Cuesta, A., Tailoring the Interfacial Water Structure by Electrolyte Engineering for Selective Electrocatalytic Reduction of Carbon Dioxide. *ACS Catalysis* **2023,** *13* (13), 8384-8393.

29. Chen, X.; Wang, X.-T.; Le, J.-B.; Li, S.-M.; Wang, X.; Zhang, Y.-J.; Radjenovic, P.; Zhao, Y.; Wang, Y.-H.; Lin, X.-M.; Dong, J.-C.; Li, J.-F., Revealing the role of interfacial water and key intermediates at ruthenium surfaces in the alkaline hydrogen evolution reaction. *Nat. Commun.* **2023,** *14* (1), 5289.

30. Li, M.; Li, L.; Huang, X.; Qi, X.; Deng, M.; Jiang, S.; Wei, Z., Platinum–Water Interaction Induced Interfacial Water Orientation That Governs the pH-Dependent Hydrogen Oxidation Reaction. *J. Phys. Chem. Lett.* **2022,** *13* (45), 10550-10557.

31. Li, J.; Li, X.; Gunathunge, C. M.; Waegele, M. M., Hydrogen bonding steers the product selectivity of electrocatalytic CO reduction. *Proc. Natl. Acad. Sci. U.S.A.* **2019,** *116* (19), 9220-9229.

32. Fejzić, H.; Kumar, R.; Gomes, R. J.; He, L.; Houser, T. J.; Kim, J.; Mohebi, M.; Molten, N.; Amanchukwu, C. V., Water Clustering Modulates Activity and Enables Hydrogenated Product Formation during Carbon Monoxide Electroreduction in Aprotic Media. *J. Am. Chem. Soc.* **2025,** *147* (22), 18445-18459.

33. Ringe, S.; Morales-Guio, C. G.; Chen, L. D.; Fields, M.; Jaramillo, T. F.; Hahn, C.; Chan, K., Double layer charging driven carbon dioxide adsorption limits the rate of electrochemical carbon dioxide reduction on Gold. *Nat. Commun.* **2020,** *11* (1), 33.

34. Edington, S. C.; Gonzalez, A.; Middendorf, T. R.; Halling, D. B.; Aldrich, R. W.; Baiz, C. R., Coordination to lanthanide ions distorts binding site conformation in calmodulin. *Proc. Natl. Acad. Sci. U.S.A.* **2018,** *115* (14), E3126-E3134.

35. Valentine, M. L.; Waterland, M. K.; Fathizadeh, A.; Elber, R.; Baiz, C. R., Interfacial Dynamics in Lipid Membranes: The Effects of Headgroup Structures. *J. Phys. Chem. B* **2021,** *125* (5), 1343-1350.